Cell. Mol. Life Sci. (2011) 68:2769–2784
DOI 10.1007/s00018-010-0591-4

Cellular and Molecular Life Sciences

RESEARCH ARTICLE

Calcium-induced cleavage of DNA topoisomerase I involves the cytoplasmic-nuclear shuttling of calpain 2

Shang-Min Chou · Ting-Hsiang Huang · Hsiang-Chin Chen · Tsai-Kun Li

Received: 31 March 2010 / Revised: 29 October 2010 / Accepted: 2 November 2010 / Published online: 18 November 2010

Abstract Important to the function of calpains is temporal and spatial regulation of their proteolytic activity. Here, we demonstrate that cytoplasm-resident calpain 2 cleaves human nuclear topoisomerase I (hTOP1) via Ca^{2+}-activated proteolysis and nucleoplasmic shuttling of proteases. This proteolysis of hTOP1 was induced by either ionomycin-caused Ca^{2+} influx or addition of Ca^{2+} in cellular extracts. Ca^{2+} failed to induce hTOP1 proteolysis in calpain 2-knockdown cells. Moreover, calpain 2 cleaved hTOP1 in vitro. Furthermore, calpain 2 entered the nucleus upon Ca^{2+} influx, and calpastatin interfered with this process. Calpain 2 cleavage sites were mapped at K^{158} and K^{183} of hTOP1. Calpain 2-truncated hTOP1 exhibited greater relaxation activity but remained able to interact with nucleolin and to form cleavable complexes. Interestingly, calpain 2 appears to be involved in ionomycin-induced protection from camptothecin-induced cytotoxicity. Thus, our data suggest that nucleocytoplasmic shuttling may serve as a novel type of regulation for calpain 2-mediated nuclear proteolysis.

Keywords Calpain · Topoisomerase · Proteolysis · Calcium · Nucleocytoplasmic shuttling

Abbreviations

Ca^{2+}	Calcium ion
ER	Endoplasmic reticulum
CAPN1/2	Calpain 1/2
hTOP1	Human DNA topoisomerase I
$hTOP1^{tr}$	Truncated hTOP1
FAK	Focal adhesion kinase
DRB	5,6-Dichloro-1-β-d-ribofuranosylbenzimidazole
BAPTA	1,2-Bis (o-amino-phenoxy) ethane-N, N, N′, N′-tetraacetic acid
CHX	Cycloheximide
Lac	Lactacystin
CAPN Inh I	Calpain inhibitor I
CAPS Inh VI	Caspase inhibitor VI
IFA	Immunofluorescence assay
GST	Glutathione-S-transferase
siRNA	Small interference RNA
CPT	Camptothecin
hTOP1 cc	HTOP1 cleavable complex

Introduction

Successful tight control of cellular proteolytic systems is crucial for maintaining cellular homeostasis. Abnormal activation of proteolytic systems has been observed in diseases and is implicated in the pathogenesis of such as muscle wasting [1] and neurodegenerative diseases [2–4]. Similarly, the impaired homeostasis of the calcium ion (Ca^{2+}) is associated with various pathological states, such as muscular atrophies [5, 6] and ischemia [3, 7]. The Ca^{2+} imbalance resulting from endoplasmic reticulum (ER) stress and/or dysfunction of Ca^{2+} channels often leads to

Electronic supplementary material The online version of this article (doi:10.1007/s00018-010-0591-4) contains supplementary material, which is available to authorized users.

S.-M. Chou · T.-H. Huang · H.-C. Chen · T.-K. Li (✉)
Department and Graduate Institute of Microbiology, College of Medicine, Taipei, Taiwan
e-mail: tsaikunli@ntu.edu.tw

T.-K. Li
Center for Biotechnology, National Taiwan University, Taipei, Taiwan

the activation of proteolytic enzymes [8–10], which are mainly performed by the calpain family proteases [11–13]. Interestingly, calpains are also implicated in the pathogenesis of Alzheimer's disease [2], sarcopenia [5, 6], and tumor progression [14–17], which has been attributed mostly to their proteolytic cleavage of cytosolic and membrane proteins. However, the potential mechanism(s) of action and biological importance of calpain-mediated cleavage of nuclear proteins remain to be investigated.

Mammalian cells have 14 members of the calpain family. Some (e.g., calpain 1, 2, 5, 7, 10, 13, and 15) are ubiquitous enzymes, whereas others (e.g., calpain 3, 6, 8, 9, 11, and 12) are confined to specific tissues [18]. Among them, calpain 1 and 2 (μ- and m-calpain; CAPN1 and CAPN2) are the best characterized. These two proteases require Ca^{2+}, but display differential sensitivities in Ca^{2+} concentrations ($[Ca^{2+}]$), for in vitro activation using purified enzymes [13]. In the presence of Ca^{2+}, autolysis of calpain 1 occurs at the N′-termini of both subunits, resulting in a reduced $[Ca^{2+}]$ requirement for activation and providing additional regulation of its calpain activity [11, 12, 19]. Another central regulatory mechanism involves the natural inhibitor calpastatin, which has been shown to inhibit protease activity by binding to both subunits of calpain in the cytoplasm [20–25]. Moreover, localizations of calpains are also involved in their regulation [18]. In this regard, calpain 2 has been shown to be present in the cytoplasm and nuclear compartments of mouse myogenic cells and is implicated in the control of the cell cycle [26, 27]. Despite the above reports, the potential regulatory mechanisms by which calpains are activated, especially in the nucleus, remain poorly defined.

Calpain proteases hydrolyze most of their substrates in a limited proteolysis manner and subsequently lead to alterations in biochemical activities rather than loss of function and/or degradation of substrates [28]. These calpain-mediated alterations in the activities of targeting substrates are thus mainly responsible for all observed cellular phenotypes and pathological conditions associated with abnormal calpain activation. For example, through proteolysis of cytoskeletal talin and vinculin proteins as well as the signaling FAK kinase, calpains may be involved in the remodeling of the cytoskeleton anchorage complex and the regulation of cell adhesion, migration, and fusion [29–32]. Notably, many calpain substrates (e.g., FAK and talin) identified in vitro are located either in the cytoplasm or on the membrane, which is in agreement with the primarily cytoplasmic location of these proteases [31, 32]. However, a few recent reports have revealed that proteins in the nuclear pore complex or nucleus itself are potential calpain substrates, thereby suggesting the potential nuclear functions of calpains [33]. The underlying mechanism(s) and regulation(s) of the calpain-mediated cleavage of nuclear proteins thus require further investigation.

DNA topoisomerases belong to a ubiquitous family of nuclear enzymes functioning in all aspects of DNA-tracking processes, such as DNA replication, RNA transcription, and recombination repair [34]. Based on their catalytic mechanisms, these enzymes can be further categorized into two types: type I (TOP1) and type II topoisomerases (TOP2) [35, 36]. Both human TOP1 (hTOP1) and hTOP2 have been proven to be therapeutic targets for anticancer therapy [37, 38]. Clinically useful camptothecin (CPT) induces cell killing via the formation of hTOP1 cleavable complexes (hTOP1 cc) [39]. Here, we report that the nucleocytoplasmic shuttling of cytosolic calpain 2 contributes to its Ca^{2+}-activated proteolysis of hTOP1. Pharmacological inhibitor and RNA interference experiments suggest that calpain 2 plays an important role in this Ca^{2+}-activated hTOP1 proteolysis. Using in vitro fractionation and reconstitution approaches, our results revealed that Ca^{2+} activated cytosolic protease(s) to cleave hTOP1 and that the nuclear membrane served as a barrier against the access of calpain 2 to hTOP1 proteins. We also observed that Ca^{2+} influx not only activates the proteolytic activity of calpain 2 but also promotes its nuclear entry. Interestingly, the natural inhibitor calpastatin reduced Ca^{2+}-activated cleavage of hTOP1 by restricting calpain 2 in the cytoplasm, whereas catalytic inhibitors had no effect on the nuclear entry of calpain 2. Calpain 2-mediated cleavage sites were further mapped at N-terminal K^{158} and K^{183} of hTOP1. The resulting N-terminus-truncated hTOP1 ($hTOP1^{tr}$) proteins exhibit greater relaxation activity but retain its ability to be poisoned by CPT and to interact with nucleolins. Furthermore, this calpain 2-mediated hTOP1 proteolysis seemed to be associated with ionomycin-mediated protection from CPT-induced cell killing. In sum, we have found a mechanism of action for calpain 2 in which this protease cleaves nuclear hTOP1. This calpain 2-mediated hTOP1 proteolysis not only impacts its biochemical activities but also alters some cellular functions of hTOP1. Additionally, a novel regulatory mechanism of calpastatin on the nuclear proteolytic activity of calpain 2 has also been suggested.

Materials and methods

Drugs, chemicals, reagents, and cell cultures

5, 6-Dichloro-1-β-d-ribofuranosylbenzimidazole (DRB), 1, 2-bis (o-amino-phenoxy) ethane-N, N, N′, N′-tetraacetic acid (BAPTA), caspase inhibitor VI, calpain inhibitor I/II, lactacystin, calpain 1 (from human erythrocytes) and calpain 2 (rat, recombinant) were purchased from Calbiochem. Other chemicals were obtained from Sigma. The HCT116 colorectal cancer cell line was a generous gift

from Dr. L.F. Liu (Univ. Med. Den. NJ, USA). The AGS gastric, MCF7 breast, HT29 and SW480 colorectal cancer cell lines were from Drs. M-C Huang and J-T Wang (National Taiwan Univ. College of Med, NTUCM, Taiwan).

Antibodies, immunoblotting, and immunofluorescence

Antibodies against eEF1α, hTOP1 N′-terminal 100–200 a.a. ($TOP1_{\alpha\text{-Nt}}$) and nucleolin were generous gifts from Drs. S. Chang, S–C Lu (NTUCM, Taiwan), J. Hwang (Academia Sinica, Taiwan) and S.H. Yoshimura (Kyoto U, Japan). Antibodies against hTOP2α (sc-13058), calpain 1 (sc-13990) and hTOP1 C′-terminus ($TOP1_{\alpha\text{-Ct}}$) (sc-5342) were from Santa Cruz Biotech. Antibodies against GADPH (H86504 M) and hTOP1 central region 400–600 a.a. ($TOP1_{\alpha\text{-Cn}}$) (ab3825) were purchased from Biodesign and Abcam, respectively. PARP1 (556362, BD Biosciences) and calpain 2 antibodies (3372-100, BioVision, for immunoblotting assay & 208727, Calbiochem, for immunofluorescence analysis) were obtained commercially. The immunoblotting assays were performed as previously described (number of replicates, $n = 2$ or 3) [40]. All antibodies in immunoblotting analyses were used at a ratio of 1:1,000 except for anti-$TOP1_{\alpha\text{-Nt}}$ and anti-GAPDH antibodies, which were used with 5,000× and 50,000× dilutions, respectively.

For the immunofluorescence assay ($n = 3$), HCT116 cells were plated onto cover slips (coated with FBS) a day before drug treatments. Drug-treated cells were washed with PBS and then fixed with 3% paraformaldehyde and 2% sucrose in PBS. After 10-min fixation at room temperature and three PBS washes, cells were permeated via an incubation in buffer A (20-mM HEPES, 50-mM NaCl, 3-mM $MgCl_2$, 300-mM sucrose and 0.5% Triton X-100) at room temperature for 10 min. Cover slips were washed with PBS, blocked in buffer B (5% FBS and 0.05% Tween-20 in PBS) for 3 h and incubated with primary antibodies in buffer B for another 16 h at 4°C. After washing three times with PBS, cells were incubated with AlexaFluor488- or Rhodamine-conjugated secondary antibodies (Molecular Probes) in Hoechst 33342 (10 μM)-containing buffer B at 37°C for an hour. After the PBS washes, the cells were then mounted in Fluoromount-G (Southern Biotechnology Associates). Images were captured with a TCS SP2 confocal microscope (Lecia) equipped with a CCD camera (Optronics) or an epi-fluorescence microscope (Nikon Eclipse 80i) with a CCD camera (Nikon DS-Ri1). Hoechst DNA staining was used to indicate the location of the nucleus. Typically, images of nuclear staining were scanned with 14 sections along the *Z* axis with an objective lens (HCX PL APO 63.0 × 1.32 OIL PH3 UV) for image collection after determining the edges of the cells. After initial localization of the nucleus by Hoechst staining, the representative images for nuclear staining of calpain 2 were directly scanned/captured in the single section with the largest nuclear diameter.

In vitro protease activation assay

The protease activation assay was performed similar to the published procedure for the calpain activation assay [41]. Briefly, 2×10^7 HCT116 cells were washed with PBS twice and cells were then lysed directly with 200 μl of a calpain activation buffer containing 50-mM NaCl, 10-mM EGTA, 0.1% Triton X-100 and 100-mM HEPES (pH 7.5). Different divalent cations (5-mM Ca^{2+}, Mg^{2+}, or Mn^{2+}) with or without 10-mM EGTA were added to activate proteases ($n = 1$ using $TOP1_{\alpha\text{-Nt}}$ antibodies, $n = 1$ using $TOP1_{\alpha\text{-Ct}}$ antibodies). After a 10-min incubation at room temperature, reactions were stopped by the sample buffer (50-mM Tris–HCl pH 6.8, 2% SDS, 0.1% Bromophenol Blue, 10% glycerol and 0.1-M β-mercaptoethanol). Immunoblotting analysis was performed to analyze the integrity of hTOP1 proteins.

Nuclei isolation and cellular fractionation

HCT116 cells ($\sim 5 \times 10^6$) were pelleted and washed twice with PBS. The cell pellet was then re-suspended in 200 μl of hypotonic buffer (10-mM Tris–HCl pH 7.9, 140-mM KCl, 5-mM $MgCl_2$, and 1-mM DTT). After a 5-min incubation on ice, NP40 (0.25%) was added to the cell mixtures with an additional 3-min incubation and then followed with gentle taps to break down cellular membrane. The supernatant was collected as cytoplasmic extract after a 5-min centrifugation at $800 \times g$ with a microfuge (4°C). The nucleus pellet was re-suspended with 1 ml of washing buffer (20-mM Tris–HCl pH 7.9, 140-mM KCl, and 20% glycerol), span at $800 \times g$ for 5-min and collected as the fraction of intact nuclei. To prepare the nuclear extract, isolated nuclei were dissolved in 100 μl of nuclear extraction buffer (10-mM HEPES pH 7.5, 350-mM NaCl, 5-mM EDTA, 5-mM DTT) with 30-min gentle rotation. The nuclear mixture was then subjected to centrifugation at $12{,}000 \times g$ for 10 min and the supernatants were collected as nuclear extracts ($n = 2$).

Purification of TOP1 and GST-fused TOP1 fragments

Recombinant full-length of hTOP1 proteins were expressed in a baculovirus system and purified following a published procedure [42]. Plasmids expressing different lengths of GST-fused hTOP1 fragments were obtained from Dr. E.H. Rubin (Cancer Institute of NJ, USA) [43]. After transformation of the constructs into *E. coli* BL21, bacteria were

grown at 26°C in Luria Broth containing 100 μg/ml of ampicillin and shaken until the A_{600} reached ~0.6. After 4 h of incubation with 0.5-mM isopropyl-β-D-1-thiogalactopyranoside (IPTG), the cells were harvested and then washed once with STE buffer (10-mM Tris pH 8.0, 150-mM NaCl and 1-mM EDTA). Bacteria were re-suspended in STE buffer containing 100-μg/ml lysozyme and incubated for 15 min on ice for cellular lysis. After the addition of 5-mM DTT and 1.5% N-lauryl-sarcosine, bacterial lysates were further sonicated on ice. After spinning briefly, supernatants were incubated with prepared glutathione Sepharose beads (Pharmacia) for 1 h at 4°C. The beads were washed four times with cold PBS. GST-fused proteins (e.g., GST-$TOP1_{141–166}$ containing the hTOP1 fragment from amino acid 141 to 166) were eluted with an elution buffer (10-mM reduced glutathione and 40-mM Tris pH 8.0).

Identification of calpain 2 cleavage sites in hTOP1, in vitro calpain cleavage assay and DNA relaxation analysis

Reaction mixtures in the calpain cleavage (CC) buffer (10-mM Tris pH 7.5, 50-mM NaCl, 1-mM DTT, 1-mM EDTA, and 0.1-mg/ml BSA) containing purified hTOP1 (~0.5 μg) were mixed with or without 5-mM Ca^{2+} and 0.8-U calpain 2. In these experiments, we used 0.8-U calpain to achieve a nearly complete digestion of recombinant hTOP1 and thereby optimized conditions for the in vitro assays. Reactions were stopped by the addition of EGTA (final concentration of 5 mM) after a 10-min incubation at room temperature. Reaction mixtures were subjected to both the immunoblotting assay and DNA relaxation analysis. The DNA relaxation assay was performed in a 30-μl mixture consisting of 0.5 μg of supercoiled DNA substrate (pBR322) with intact hTOP1, the $hTOP1^{tr}$-containing mixture or various cellular extracts (~20 μg) in the relaxation buffer (10-mM Tris pH 7.5, 50-mM NaCl, 1-mM EDTA, 1-mM DTT and 100 μg/ml of BSA). After a 10-min incubation at 37°C, an adequate amount of stop solution (final 1% SDS, 0.0005% Bromophenol Blue, 6% glycerol and 10 μg of protease K) was added and followed by an incubation at 37°C for 30 min. The activity of hTOP1 in relaxing DNA was analyzed with a 0.8% agarose gel with 1.2 V/cm at 4°C for 15 h in 0.5× Tris–phosphate-EDTA (TPE) buffer.

For the identification of calpain 2-cleaved sites on hTOP1, two GST-fused hTOP1 fragments (GST-$TOP1_{141–166}$ or GST-$TOP1_{166–210}$, ~1.5 μg) were subjected to the calpain cleavage assay with 0.8 U calpain 2 as described above (with the exception of a longer incubation time of 15 min). The cleavage mixtures were then loaded into Microcon YM-10 (Millipore) and spun to eliminate proteins with molecular weights (MWs) larger than 12.4 kDa (>95%, according to the manufacturer's report). Eluted samples containing non-GST-fused cleaved products were collected and delivered to Mission Biotech (Taiwan) for MALDI-TOF/mass spectrometry analysis.

Lentivirus-mediated small RNA interference (siRNA)

Knockdown of calpain 2 expression was achieved by a lentivirus-packaged siRNA approach as described previously (http://rnai.genmed.sinica.edu.tw/). Five different pLKO.1-shRNA plasmids expressing calpain 2-targeting siRNAs (siCapn2 #39–43) were obtained from the National RNAi Core Facility (Taiwan). The calpain 2-targeting sequences for siCapn2 #39 and siCapn2 #43 are listed below: GCGCTCAGACACCTTCATCAA and CCCGAG AATACTGGAACAATA. Plasmid pLKO.1-shRNA (with puromycin resistant gene), pMD.G (VSV envelope protein), and pCMVDR8.91 (gag, pol, and rev proteins) were co-transfected into 293T cells (~1.2×10^6) with a 1:0.1:1 ratio by Lipofectamine plus (Invitrogen). Culture media containing released viruses were collected every 24 h for 3 days after transfection and the viral soups were then used for viral infection. One day after separated viral infection with five different si-Capn2-expressing lentiviruses ($n = 1$), HCT116 cells were subjected to clonal selection with puromycin (2 μg/ml) for an additional 3 days. The surviving cells were then pooled and further cultivated into stable five clones (HCT116 si-Capn2 #39–43). Immunoblotting analysis with anti-calpain 2 antibodies was used to examine the knockdown efficiencies of pooled clones (data no shown for HCT116 si-Capn2 #40–42 cells). HCT116 si-Capn2 #39 and #43 cells were selected for further experiments.

The coimmunoprecipitation (CoIP) assay

Approximately 2×10^7 HCT116 cells were treated with 10-μM ionomycin for 15 min., harvested and then washed with PBS twice. After a brief spin at 13,000 × *g*, cells were lysed with calpain activation buffer containing an additional 1× protease inhibitor cocktail (Roche). Supernatants were collected after 20-min of centrifugation at 13,000 × *g*. After the addition of pre-immune mouse serum or anti-nucleolin antibodies to the collected supernatants, reaction mixtures were immediately rotated at 4°C for 1 h. Protein G-Sepharose beads were then added to the mixtures and further incubated overnight at 4°C with gentle rotation. The beads were washed once with calpain activation buffer and four times with PBS. After the addition of sample buffer, immunoblotting analyses with two kinds of antibodies against the hTOP1 ($n = 2$, with either $TOP1_{\alpha\text{-Ct}}$,

or $TOP1_{\alpha\text{-Cn}}$) or with nucleolin antibodies were carried out to determine the interaction between hTOP1 and nucleolin.

Assays for human TOP1 cleavable complex (hTOP1 cc)

For detection and characterization of hTOP1 cc and $hTOP1^{tr}$cc, 10^6 of HCT116 cells were treated with or without 5-μM ionomycin for 15 min and co-incubated with CPT (5 μM) for another 30 min at 37°C. For the band depletion assay [40], the drug-treated cells were lysed with alkaline lysis and then subjected to immunoblotting analysis to examine CPT-induced formation of hTOP1 cc and/or $hTOP1^{tr}$cc. In the medium reversal experiments, an additional incubation in CPT-free media 30 min prior to lysis was carried out to determine the reversible nature of hTOP1 cc and $hTOP1^{tr}$cc. The alkaline lysis was performed with one appropriate volume of alkaline lysis buffer (0.2-N NaOH, 2-mM EDTA), which was then neutralized with a 1/10 volume of 10× neutralization solution (10% NP-40, 1-M Tris pH 7.4, 100-mM $MgCl_2$, 100-mM $CaCl_2$, 10-mM dithiothreitol, 1-mM EGTA, and a protease inhibitor cocktail) with a 1/10 volume of 2 N HCl. For the release of hTOP1 cc or $hTOP1^{tr}$cc from chromatin DNA, neutralized cell lysates were further incubated with *S. aureus* DNA nuclease S7 (60 U per reaction) on ice for 30 min. Reactions were terminated using sample buffer.

Colony formation assay

The clonogenic assay was performed as described ($n = 3$) [40] to examine the potential effect of ionomycin on CPT-induced cell killing. Sub-confluent cells were pre-treated with or without 5-μM ionomycin for 15 min and then co-treated with or without CPT for another 30 min. Drug-treated cells ($4–8 \times 10^2$ per plate) were re-seeded onto 60-mm culture dishes with drug-free medium. Surviving cells were allowed to grow into colonies in a 5% CO_2 incubator at 37°C for 12 days. Colonies were stained (with 0.03% crystal violet and 2% ethyl alcohol) and scored.

Quantitative and statistical analyses

Immunoblotting results were scanned and saved as electronic files. The intensities of individual bands were then graphed and determined with the ImageQuant program (Molecular Dynamics). In the medium reversal and S7-release experiment, the level of free $hTOP1^{tr}$ protein in the ionomycin-treated sample was taken as 100%. For the quantitative analysis of IFA results, both nuclear staining of calpain 2 and nucleolar enrichment of hTOP1 were scored as positive ones from several fields of confocal microscope images (up to ~50 or 100 cells/per field). In control cells, hTOP1 proteins locate in both nucleoplasm and nucleoli. After ionomycin treatments, cells with a much reduced immunofluorescent signal of hTOP1 in nucleoplasm compartment and increased hTOP1 signals in nucleoli were scored as positive in nucleolar enrichment of hTOP1. Statistical analysis for differences between the numbers of survival rates, protein levels of hTOP1 and calpain 2, percentage values of hTOP1 proteolysis and nuclear calpain 2 staining was performed with Student's *t* test. Data were considered statistically significant when *p* values were <0.05 and <0.01, which are shown with single (*) and double asterisks (**), respectively.

Results

Ionomycin treatment induces rapid and Ca^{2+}-dependent proteolysis of human DNA topoisomerase I (hTOP1)

Different cells were treated with Ca^{2+} ionophores and immunoblotting analysis was used to examine the effect of Ca^{2+} influx on the protein integrity of hTOP1. In Fig. 1a, cellular exposure to 10-μM ionomycin caused limited proteolysis of hTOP1 in four different cell lines with different efficiencies but not in SW480 cells (see quantitative results in Fig. 1b). Using another Ca^{2+} ionophore (A23187), similar proteolysis of hTOP1 was also observed (Fig. S1A). In addition, this ionophore-induced hTOP1 proteolysis was time- and dosage-dependent (HCT116 cells, Figs. 1c, S1A, and B). Notably, HT29 cells exhibited the highest basal level of hTOP1 proteolysis (23.8 ± 4.8%, Fig. 1b) among the five cell lines examined. Interestingly, similar cleavage products were observed in ionomycin-treated HCT116 cells using different hTOP1 antibodies ($TOP1_{\alpha\text{-Nt}}$ for the N′-terminus, $TOP1_{\alpha\text{-Cn}}$ for the central domain and $TOP1_{\alpha\text{-Ct}}$ for the C′-terminus). Furthermore, the proteolytic sites of hTOP1 are likely located within its N′-terminal 200 amino acids according to the epitope specificity of TOP1 antibodies (Fig. 1d).

To confirm the contribution of intracellular [Ca^{2+}] to the above hTOP1 proteolysis effect of ionomycin, we took advantage of the Ca^{2+} chelator EGTA. As shown in Fig. 1e, 2-mM EGTA abolished the ionomycin-induced proteolysis of hTOP1. Moreover, extracellular addition of Ca^{2+} in culture media also caused a dose-dependent hTOP1 proteolysis in HCT116 cells (Fig. 1f), providing further support for the direct role of Ca^{2+} in this limited proteolysis of hTOP1. Consistently, co-treatment of cells with 5-mM Ca^{2+} and 20-μM ionomycin caused a significant increase in hTOP1 proteolysis (~52%) compared to HCT116 cells treated with 20-μM ionomycin only (~25%). No hTOP1 proteolysis was observed in the presence of additional 10-mM EGTA (Fig. 1g). The

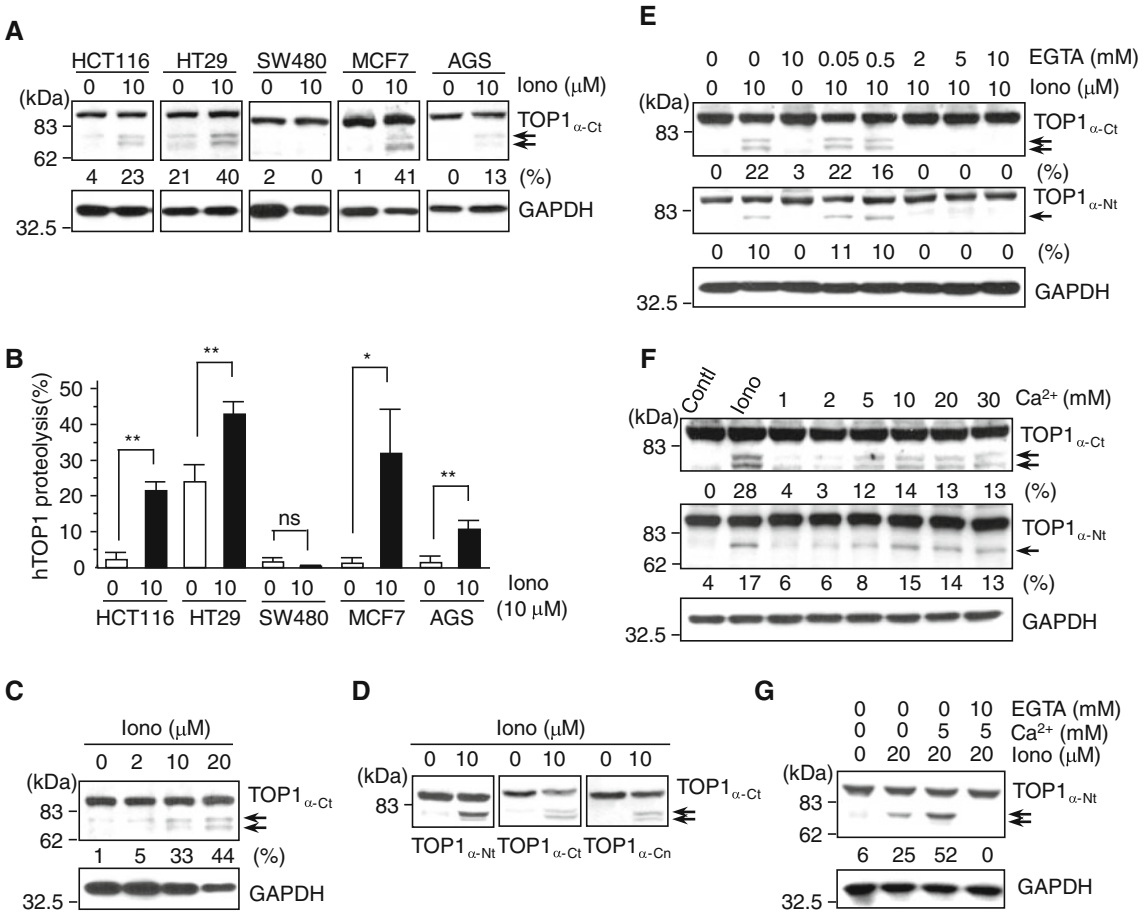

Fig. 1 Ionomycin treatment induced rapid, but limited proteolysis of human DNA topoisomerase I (hTOP1) in cells. **a** Cellular exposure to ionomycin resulted in the cleavage of hTOP1 proteins in various cell lines. HCT116, HT29, SW480 colorectal, MCF7 breast and AGS gastric cancer cells were treated with or without ionomycin (Iono, 10 μM) for 15 min, harvested and lysed. Equal amounts of different cell lysates were subjected to immunoblotting analysis with antibodies against the C-terminus of TOP1 ($TOP1_{\alpha\text{-}Ct}$) and GAPDH (as the loading control) and proteolysis results were quantified (number of replicates, $n = 3$) (**b**). **c** Ionomycin-induced hTOP1 proteolysis is dose-dependent. **d** The proteolysis of hTOP1 induced by ionomycin is likely caused by the protease-mediated cleavage at the N′-terminus. HCT116 cells were treated with ionomycin (doses as indicated) and the integrity of proteins was analyzed as described in **a**. Antibodies against the central domain, N-terminus, and C-terminus of hTOP1 (named $TOP1_{\alpha\text{-}Cn}$, $TOP1_{\alpha\text{-}Nt}$, and $TOP1_{\alpha\text{-}Ct}$, respectively) were used for the epitope-mapping of potential proteolytic sites on hTOP1. **e** Ca^{2+} chelation by EGTA prevented hTOP1 proteolysis induced by ionomycin. HCT116 cells were pre-treated with EGTA for 30 min and then underwent co-treatment with ionomycin for 15 min. **f** The hTOP1 proteolysis was also observed with extracellular addition of Ca^{2+} to the culture media. Different concentrations of Ca^{2+} (as indicated on the top of figure) were add directly into the media and HCT116 cells were further incubated for 15 min. **g** The addition of extracellular Ca^{2+} also greatly stimulated ionomycin-induced proteolysis of hTOP1. HCT116 cells were treated with different combinations of 5-mM Ca^{2+}, 10-mM EGTA (pre-treatment for 30 min) and 20-μM ionomycin for 15 min. Cells were lysed, and immunoblotting analyses were carried out as described above. *Arrows* indicate the truncated hTOP1 fragments. $^{**}p < 0.01$; $^{*}p < 0.05$; *ns*, statistically non-significant

specific involvement of Ca^{2+} was further supported by the observation that only 5-mM Ca^{2+}, but not an equal concentration of other cations (i.e., 5 mM), triggered hTOP1 proteolysis in total cell lysates (Fig. 2a, immunoblotting analysis with $TOP1_{\alpha\text{-}Nt}$ antibodies). Similar conclusion was also obtained by the same in vitro protease activation assay using total cell lysates coupled with immunoblotting analysis using $TOP1_{\alpha\text{-}Ct}$ antibodies (data not shown). In sum, our data suggest that Ca^{2+} influx activates the limited proteolysis of nuclear hTOP1.

Cytosolic calpain proteases, but not caspases or the proteasome, contribute to Ca^{2+}-activated hTOP1 proteolysis

Next, we sought to identify the protease(s) responsible for this Ca^{2+}-activated hTOP1 proteolysis. The fractionation and reconstitution approaches as well as the in vitro cleavage assay were first used to identify and localize the responsible protease(s). In Fig. 2b, we found that the Ca^{2+}-activated hTOP1 proteolysis could only occur when

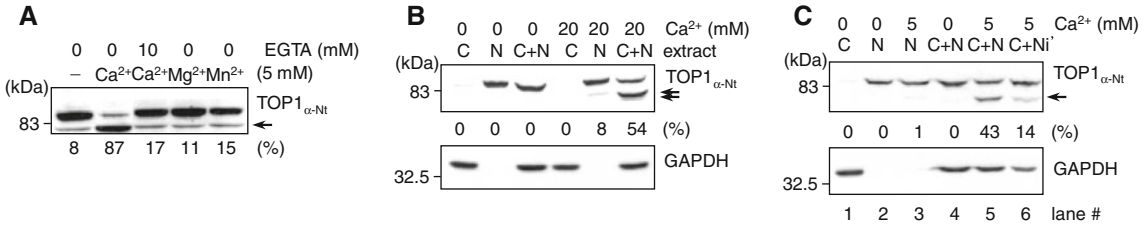

Fig. 2 In vitro proteolytic cleavage of nuclear hTOP1 by Ca^{2+}-activated cytosolic proteases. **a** Ca^{2+}, but not Mg^{2+} or Mn^{2+}, effectively activated hTOP1 proteolysis in HCT116 cell extracts. The in vitro protease activation assay using total extracts was performed in the absence or presence of different divalent cations (5 mM) as described in "Materials and methods". **b** The fraction and reconstitution experiments revealed that cytosolic extract contains the Ca^{2+}-activated proteolytic activity on hTOP1. **c** The intact nuclear membrane partially blocked the Ca^{2+}-activated cleavage of hTOP1. The Ca^{2+}-activated hTOP1 proteolytic reaction was reconstituted by various combinations of cytosolic extract (C), nuclear extract (N) and isolated nuclei (Ni′) as described in "Materials and methods" ($n = 2$). Ca^{2+} (5 mM) was added to activate the protease(s). After incubation at room temperature for 10 min, the mixtures were subjected to immunoblotting analysis with $hTOP1_{\alpha\text{-Nt}}$ antibodies

cytosolic (C) and nuclear extracts (N) were mixed together, suggesting the cytoplasmic location of the protease(s). Compared to that with the nuclear extract, a reduction in the level of hTOP1 proteolysis was observed when intact nuclei (Ni′) were combined with the Ca^{2+}-activated cytosolic fraction (Fig. 2c, compare lane 4–5). In addition, large truncated fragments of hTOP1 ($hTOP1^{tr}$) and intact hTOP1 proteins remained in the nuclear fraction (Fig. S1C), suggesting that Ca^{2+}-activated hTOP1 proteolysis likely occurs in the nucleus. The alternative experiments using the same approach, but different hTOP1 antibodies ($TOP1_{\alpha\text{-Ct}}$ antibodies), had been performed and similar observations were observed (data not shown). Collectively, these results support the notion that Ca^{2+}-activated hTOP1 proteolysis might involve the nuclear shuttling of cytosolic proteases.

The pharmacological approach using specific inhibitors was then used to examine the potential involvement of proteases. First, we found that the proteasome and caspases are likely not involved in this process, since hTOP1 proteolysis was not affected by co-treatment of either the proteasome inhibitor lactacystin (data not shown) or caspase inhibitor VI (CASP Inh VI, Fig. 3a). The calpain family included the most well-known proteases activated by Ca^{2+} [13, 18, 44]. As expected, calpain inhibitor I (CAPN Inh I) effectively blocked the ionomycin-induced hTOP1 proteolysis (Fig. 3b). Similar blockage was also observed with calpain inhibitor II (data not shown). We have also examined whether ionomycin treatment induces proteolysis of other nuclear proteins. We found that only hTOP2β and lamin A/C proteins, but not hTOP2α or PARP proteins, were cleaved into visible smaller fragments upon exposure to 10-μM ionomycin. Similarly, these proteolyses of hTOP2β and lamin A/C proteins induced by ionomycin could also be greatly diminished by either EGTA or calpain inhibitor co-treatment (data not shown).

Within the calpain family, calpain 1 and 2 are the main proteases activated by Ca^{2+} [13]. We also found that both calpain 1 and 2 were present in all five cell lines we examined (Fig. S1D). We thus examined the ability of recombinant calpain 1 and 2 to cleave purified hTOP1 proteins. In Fig. 3c, d, we observed that both calpain 1 and 2 limitedly cleaved hTOP1 into fragments with a pattern similar to that induced by ionomycin treatment in the above cell culture experiments. Recombinant calpain 2 appeared to exhibit a much higher specific cleavage activity on hTOP1 than recombinant calpain 1 (Fig. 3d). Notably, this in vitro hTOP1 proteolysis by recombinant calpain 2 was also inhibited in the presence of calpain inhibitor I or Ca^{2+}-chelating EGTA (Fig. 3e).

Calpain 2 contributes to the Ca^{2+}-activated hTOP1 proteolysis

Above in vitro experiments have identified hTOP1 as a potential substrate, that is preferentially cleaved by calpain 2 compared with calpain 1 (Fig. 3c, d). A genetic approach using RNA interference technology was employed to examine the involvement of calpain 2 in Ca^{2+}-induced hTOP1 proteolysis. Cells were infected with lentiviruses expressing different small interference RNAs specifically targeting calpain 2 (si-Capn2 #39 or #43) and then incubated in the presence of puromycin. Pooled clones of drug-resistant HCT116 cells were collected after 3 days of drug selection and further cultivated into stable lines. As shown in Fig. 3f, g, the expression of calpain 2 was knocked-down in both HCT116 si-Capn2 #39 (42.5 ± 12.0% remained) and #43 clones (17.0 ± 2.8% remained) with a greater efficiency in si-Capn2 #43 cells. Moreover, hTOP1 remained mostly intact upon exposure to 10-μM ionomycin in both HCT116 si-Capn2 #39 and #43 cells (Fig. 3h). Furthermore, knockdown of calpain 2 expression did not cause any significant change in the level of hTOP1 proteins (Fig. 3i). Together, our results thus suggest that calpain 2 is one of the protease responsible for Ca^{2+}-activated hTOP1 proteolysis.

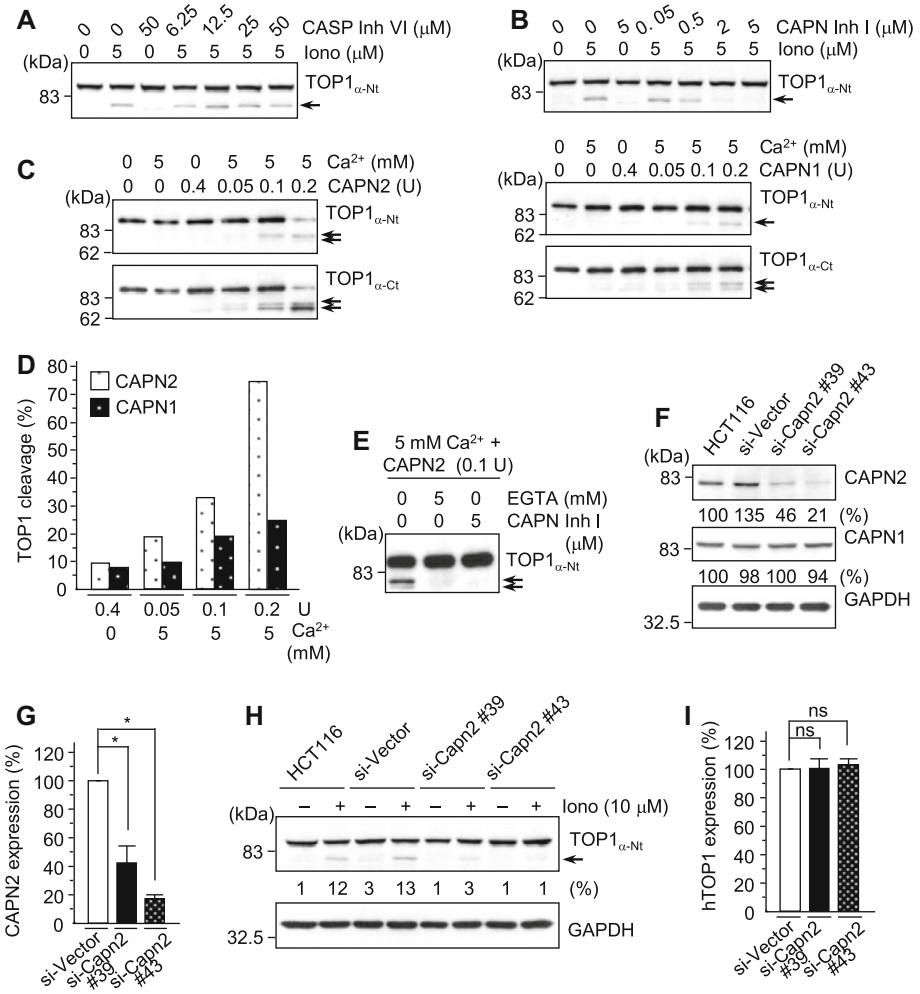

Fig. 3 Calpain 2 is the main protease responsible for the Ca^{2+}-activated proteolysis of hTOP1. **a** Ionomycin could still effectively induce hTOP1 proteolysis in the presence of caspase inhibitor. **b** Ionomycin-induced hTOP1 proteolysis was greatly reduced when calpain proteases were inhibited. Different concentrations (μM, as indicated on the *top of corresponding panels*) of caspase inhibitor VI (CASP Inh VI) and calpain inhibitor I (CAPN Inh I) were added for 30 min before ionomycin treatment (5 μM for 15 min). **c, d** The proteolysis of purified hTOP1 by recombinant calpain 1 (CAPN1) and 2 (CAPN2) in vitro. Purified calpains (human CAPN1 or rat CAPN2, at indicated units) with or without Ca^{2+} (5 mM) were mixed with recombinant hTOP1 (0.05 μg) and incubated for 10 min at room temperature; then, reactions were stopped using sample buffer. The quantitative data has been plotted in (**d**). **e** Both Ca^{2+}-chelating EGTA and calpain inhibitor I efficiently blocked in vitro proteolysis of hTOP1 mediated by the Ca^{2+}-activated recombinant calpain 2. **f, g** The expression of calpain 2 was specifically knocked-down using a RNA interference (RNAi) approach. The knockdown efficiencies in HCT116 cells of lentiviral particles expressing different shRNAs (#39 and #43) were quantified ($n = 3$) (**g**). **h** Ca^{2+}-mediated hTOP1 proteolysis was diminished in the calpain 2-deficient cells. The lentivirus-mediated RNAi approach was utilized to specifically knockdown the expression of calpain 2 in HCT116 cells. After proper selection, pooled clones of calpain 2-deficient cell lines were established. The knockdown efficiency and specificity values for these two clones (HCT116 si-Capn2 #39 and #43) are shown in (**f, g**). Ionomycin-induced hTOP1 proteolysis was then performed with two knockdown clones and HCT116 si-Vector cells as described above. **i** The expression levels of hTOP1 are not altered in two si-Capn2 cell lines ($n = 3$). * $p < 0.05$; *ns*, statistically non-significant

Nucleocytoplasmic shuttling of calpain 2 contributes to Ca^{2+}-activated hTOP1 proteolysis

The main cellular location of calpain 2 has been reported to be in the cytoplasm and most of its in vitro substrates are either membrane-associated or cytosolic proteins [28]. Consistently, we showed that calpain 2 proteins were mainly resident in the cytoplasm of untreated cells (Fig. 4a, b). Inspection of Fig. 4a reveals that a small proportion of calpain 2 re-distributed into the nuclear fraction after Ca^{2+} influx, whereas both activated and intact calpain 1 protease remained in the cytosolic fraction (Fig. 4a). In addition, nuclear staining of calpain 2 became visible after 10-μM ionomycin treatment (~28% of cells with positive nuclear staining using an epi-fluorescence microscope shown in Fig. S1E compared to 23.0 ± 0.3% of cells with positive nuclear staining using a confocal microscope shown in Fig. 4b, c). Quantitative analysis further revealed that

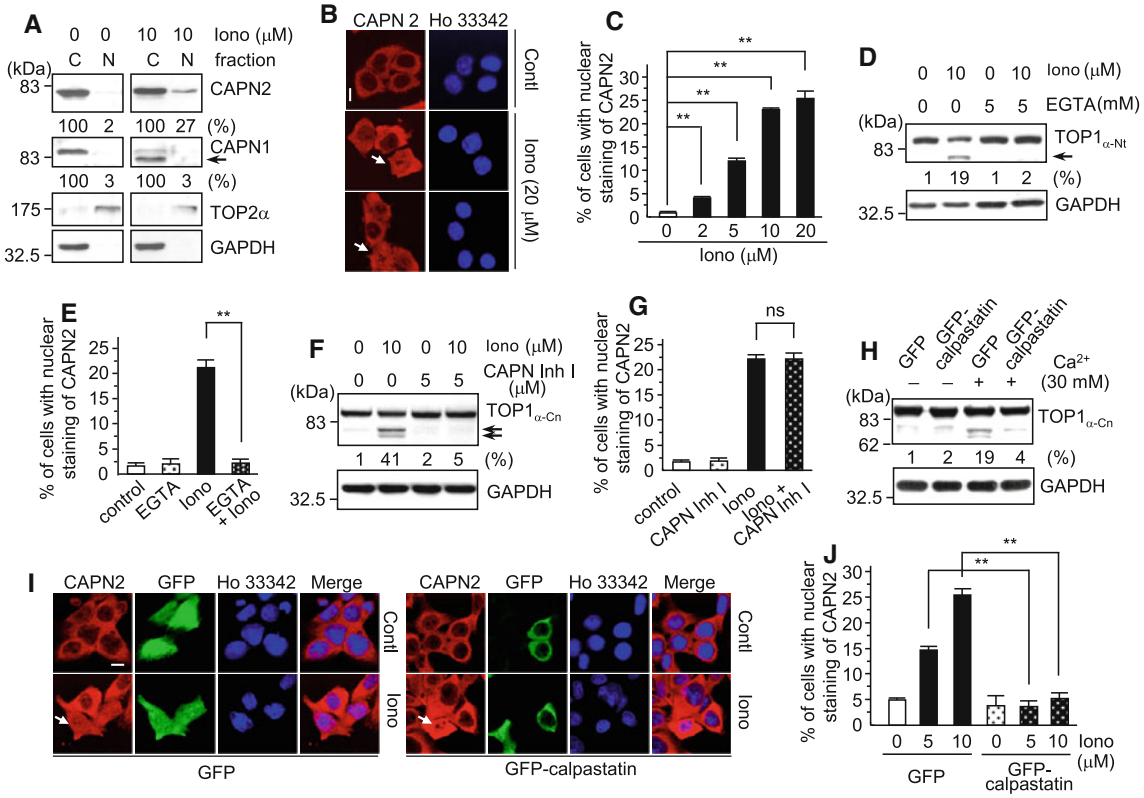

Fig. 4 Cytosolic calpain 2 entered the nucleus and cleaved hTOP1 after Ca^{2+} influx. **a**, **b** Ionomycin treatment shifted a fraction of cytoplasmic calpain 2 into the nucleus as revealed by the fractionation assay (**a**) and the immunofluorescent analysis (IFA) using a confocal microscope (**b**). Fractionation experiments were performed with HCT116 cells treated with or without ionomycin (10 μM, 15 min). Cytosolic and nuclear extracts were then analyzed by the immunoblotting analysis using anti-calpain 1 and 2 antibodies. GAPDH and hTOP2α were used as cytosolic and nuclear markers, respectively. For IFA, cells were first seeded onto cover-slips for 24 h before ionomycin treatment (20 μM for 15 min). Control and treated cells were subjected to IFA using a confocal microscope as described in "Materials and methods". Nuclear location was indicated by Hoechst 33342 staining. *Bar* 8 μM. **c** Quantitative results for the dosage dependence of ionomycin-induced nuclear entry of calpain 2 ($n = 3$). **d**, **e** Chelation of extracellular Ca^{2+} by EGTA effectively abolished both ionomycin-induced proteolysis of hTOP1 (**d**) and nuclear entry of calpain 2 ($n = 3$) (**e**). **f**, **g** Inhibition of protease activity by calpain inhibitor I (CAPN Inh I) affected only the ionomycin-induced hTOP1 proteolysis (**f**), but not the nuclear entry of calpain 2 ($n = 3$) (**g**). Ectopic expression of calpastatin reduced both Ca^{2+}-activated proteolysis of hTOP1 (**h**) and ionomycin-induced nuclear entry of calpain 2 (**i**). HCT116 cells were transfected with either a control vector or the GFP-calpastatin fusion-expressing construct. After 48 h, the GFP fluorescence assay was used to examine the transfection efficiencies (~30–40%). **j** Quantitative analysis of the effect of calpastatin expression on ionomycin-induced nuclear entry of calpain 2 ($n = 3$). Columns represent percentages of nuclei containing calpain 2 in GFP-positive cells. *White arrow heads* indicated for the cells with nuclear staining of calpain 2. $^{**}p < 0.01$; *ns*, statistically non-significant

ionomycin treatment induced nuclear entry of calpain 2 in a dosage-dependent manner (Fig. 4c). These results therefore suggest that Ca^{2+} influx not only activates the protease activity of calpain 2 but also causes its nuclear entry. Moreover, both processes are likely needed for Ca^{2+}-activated hTOP1 proteolysis.

Nuclear entry of calpain 2 is regulated by both Ca^{2+} and calpastatin, but not calpain activity

To test the above hypothesis, EGTA and calpain inhibitors were used to block Ca^{2+} influx and protease activity, respectively. As shown, EGTA abolished both proteolysis of hTOP1 (Fig. 4d) and nuclear entry of calpain 2 after ionomycin treatment (Fig. 4e). The catalytic inhibitor of calpains (CAPN Inh I) blocked the Ca^{2+}-activated hTOP1 proteolysis (Fig. 4f) but had no effect on the nucleocytoplasmic shuttling of calpain 2 (Figs. 4g and S2A). It is generally believed that the natural inhibitor calpastatin regulates the activation of calpain proteases and inhibits their catalytic activity by binding to them [23, 24, 45]. Effects of GFP-fused calpastatin on the Ca^{2+}-activated hTOP1 proteolysis and nuclear entry of calpain 2 were thus examined. As scored by the GFP-positive signal, ~30% of HCT116 cells transiently expressed calpastatin. To our surprise, calpastatin not only reduced the Ca^{2+}-activated hTOP1 proteolysis (Fig. 4h), but also blocked the ionomycin-induced nuclear entry of calpain 2 (Fig. 4i, j). With

10-μM ionomycin treatment, ectopic expression of calpastatin decreased the nuclear staining of calpain 2 from 25.3 ± 1.2% to 5.1 ± 1.0% ($p < 0.01$, Fig. 4j). Moreover, the reduction effect of calpastatin on Ca^{2+}-activated or ionomycin-induced hTOP1 proteolysis has also been observed using the same approach (as Fig. 4h) but with $TOP1_{\alpha\text{-Nt}}$ antibodies for immunoblotting analyses (data now shown). Our results thus suggest a novel role for calpastatin in regulating the Ca^{2+}-activated nuclear entry of calpain 2.

Calpain 2 cleaves hTOP1 at two N′-terminal lysine residues, K^{158} and K^{183}

The above epitope mapping results (Fig. 1d) suggest that hTOP1 proteolysis by calpain 2 likely occurs within its N′-terminal 200 amino acids. To further determine the cleavage sites, various GST-fused recombinant hTOP1 fragments were purified for the in vitro calpain 2 cleavage assay. As shown in Fig. 5a, two bacterially expressed GST-fused TOP1 proteins, $GST\text{-}TOP1_{141–166}$ (the TOP1 fragment containing amino acid 141–166) and $GST\text{-}TOP1_{166–210}$ were purified to nearly homogeneity (upper panel with Coomassie staining). Treatment of calpain 2 and Ca^{2+} caused proteolysis of both the $GST\text{-}TOP1_{141–166}$ and $GST\text{-}TOP1_{166–210}$ fragments, but not the GST proteins alone (Fig. 5a). Reaction mixtures containing cleaved products were loaded into Microcon YM-10 columns, and the flow-through parts were then collected for molecular weight (M.W.) determination by MALDI-TOF mass spectrometry analysis. In Fig. 5b, the truncated hTOP1 peptides in the flow-through part of the $GST\text{-}TOP1_{141–166}$/calpain 2/$Ca^{2+}$ eluents produced a major peak at position 1633.583 M/Z (arrow #1,

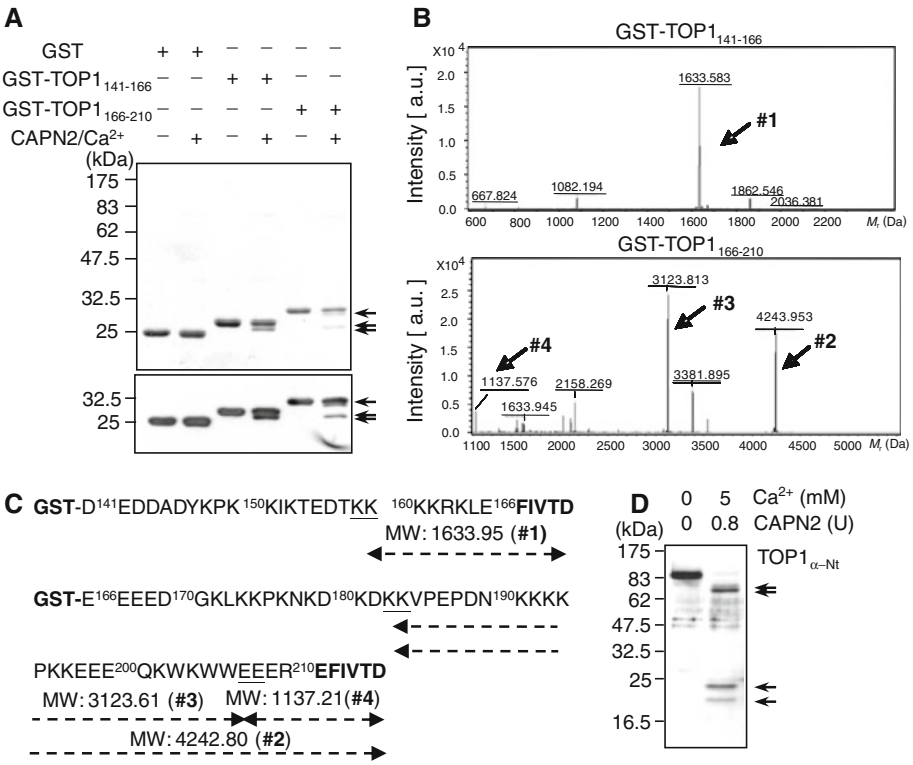

Fig. 5 Identification of the calpain 2-dependent cleavage sites in hTOP1 by mass spectrometry. **a** Purified hTOP1 fragments were cleaved by calpain 2 in vitro. **b** MALDI-TOF/MS analysis results for the calpain 2-cleaved products of GST-tagged hTOP1 fragments. Two GST-fused hTOP1 fragments, $GST\text{-}TOP1_{141–166}$ and $GST\text{-}TOP1_{166–210}$ proteins (with amino acid 141–166 and 166–210 of hTOP1, respectively), were expressed and purified from bacteria. The calpain 2 proteolytic reactions were performed with these two GST-fused tagged hTOP1 fragments and the reaction mixtures were then subjected to SDS-PAGE separation (**a**, *upper panel*; stained with Coomassie Blue), immunoblotting analysis with anti-GST antibodies (**a**, *lower panel*) and MALDI-TOF/MS analysis (**b**). The calpain 2-truncated products, the intact and truncated GST-containing hTOP1 fragments in the reaction mixtures were loaded into Microcon YM-10 columns. The flow-through parts were collected for molecular weight determination by MALDI-TOF mass spectrometry analysis. The molecular masses determined for the calpain 2-cleaved hTOP1 short fragments in the flow-through are shown underlined on the top of the peaks (**b**, units = Da). **c** Schematic mapping containing hTOP1 amino acid sequences of $GST\text{-}TOP1_{141–166}$ and $GST\text{-}TOP1_{166–210}$ peptides and the theoretical molecular masses for the calpain 2-cleaved fragments (*arrows* #1–4 shown in **b**). The non-hTOP1-derived amino acids FIVTD and EFIVTD (in *bold*) are encoded from the backbone of the pGEX-1λ-T vector after cloning, and the two calpain 2 cleavage sites in hTOP1 are underlined. **d** Calpain 2 cleaved hTOP1at two sites to produce in four fragments. After the in vitro calpain 2 cleavage of hTOP1, the reaction mixtures were subjected to immunoblotting analysis. The *arrow heads* indicate the cleaved hTOP1 fragments. *MW*, molecular weight; *a.u.*, arbitrary units

upper panel), and those from the GST-TOP1$_{166–201}$/calpain 2/Ca^{2+} eluents showed three major peaks at 4243.953, 3123.813, and 1137.576 M/Z (arrow #2, 3 and 4, lower panel). Based on the above data and theoretical calculation (Fig. 5c), we thus concluded that calpain 2 cleaves hTOP1 at its N′-terminal K^{158} and K^{183}. The cleavage site at the E^{207} is most likely due to the additional six amino acids generated from cloning. Consistently, we used the polyclonal antibodies against hTOP1$_{100–200}$ fragment (TOP1$_{\alpha\text{-Nt}}$) and showed that the more complete cleavage of recombinant hTOP1 by higher unit of calpain 2 (0.8 U) resulted in four proteolytic products with MWs of ~18, 21, 69, and 72 kDa (Fig. 5d). Together, our results suggest that calpain 2 cleaves hTOP1 at the N′-terminal K^{158} and K^{183} residues.

Ionomycin treatment induces proteolysis and translocation of hTOP1 without compromising its interaction with nucleolin

Two calpain 2 cleavage sites ($K^{158, 183}$), three caspase cleavage sites ($D^{123, 146, 170}$) and the nucleolin-interacting domain (amino acid 166–210) located on the N′-terminus of hTOP1 are illustrated in Fig. 6a. Since the calpain 2 cleavage sites, K^{158} and K^{183}, are located within the nucleolin-binding domain of hTOP1 [43], we examined the interaction between calpain 2-truncated hTOP1^{tr} proteins and nucleolin using an immunocoprecipitation approach. Interestingly, not only hTOP1 but also two large fragments of calpain 2-truncated hTOP1 (hTOP1^{tr}) were all co-precipitated by anti-nucleolin antibodies (Fig. 6b, right panel, lane 2 and 4). Therefore, calpain 2-mediated hTOP1 proteolysis does not disrupt the interaction between hTOP1 and nucleolin, further suggesting hTOP1$_{183–210}$ as the nucleolin-interacting domain.

We also examined the cellular localization of hTOP1 after ionomycin treatment. As reported [46–48], hTOP1 proteins concentrate in nucleoli with a diffuse pattern in the nucleoplasm (Fig. S2B). Nucleolin staining indicates the nucleolar location. As shown in Figs. 6c and S2B (lower left panel, indicated by the arrowhead), hTOP1 proteins seem to be more concentrated in the nucleoli after ionomycin treatment (62.0 ± 4.0% in HCT116 si-Vector cells, $n = 3$). This ionomycin-induced change of hTOP1 location is likely independent of calpain 2, since it also occurs efficiently in HCT116 si-Capn2 #43 cells (58.1 ± 2.2%, Figs. 6c and S2C).

hTOP1^{tr} proteins exhibit greater relaxation activity

The above results suggest that a part of the regulatory N′-terminus of hTOP1 is truncated by calpain 2. We examined the specific relaxation activity of the intact hTOP1 (hTOP1$_{1–765}$) and hTOP1^{tr} (hTOP1$_{158–765}$ and hTOP1$_{183–765}$) proteins. In Fig. 7a, addition of 5-mM Ca^{2+} and 0.8-U calpain 2 triggered autolysis of the protease and complete proteolysis of recombinant hTOP1. Different reaction mixtures were then diluted 2-fold and the relative activities of diluents relaxing supercoiled (SC) DNA were compared. Interestingly, the DNA relaxation activity of the hTOP1-containing mixture was increased (by roughly two-fold) when Ca^{2+} and calpain 2 were both presented (Fig. 7b).

To support the above finding, we treated HCT116 si-Vector or si-Capn2 #43 cells with ionomycin (20 μM) and then collected their extracts for immunoblotting analysis and the DNA relaxation assay. Ionomycin treatment activated proteolysis of hTOP1 in HCT116 si-Vector cells (Fig. 7c), and thus the derived cell extract is regarded as

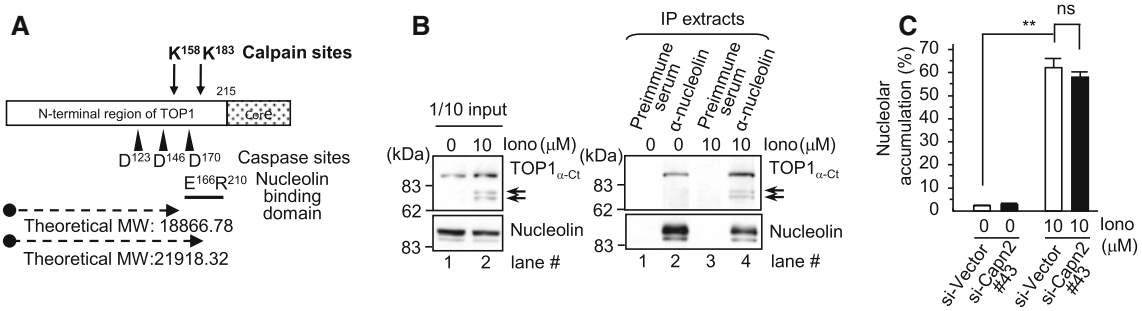

Fig. 6 Ionomycin treatment enhanced the nucleolar distribution of hTOP1, and calpain 2-mediated proteolysis of hTOP1 did not disrupt its interaction with nucleolin. **a** Diagram indicating two calpain 2 cleavage sites, three caspase cleavage sites and the nucleolin-interacting domain identified on the N-terminus of hTOP1. The two calpain 2 cleavage sites (K^{158} and K^{183}) mapped in this study and three caspase cleavage sites (D^{123}, D^{146} and D^{170}) are indicated by the *arrows* and *arrowheads*, respectively. The nucleolin-binding domain (E^{166} to R^{210}) of hTOP1 is also presented. **b** Full-length hTOP1 and calpain 2-truncated hTOP1^{tr} both interacted with nucleolin. Ionomycin-treated or control HCT116 cell lysates were subjected to the immune-precipitation (IP) assay as described using antibodies against nucleolin. **c** Nucleolar accumulation of hTOP1 is regulated by Ca^{2+} influx, but independent of calpain 2. HCT116 si-Vector and si-Capn2 #43 cells were seeded on cover-slips for 24 h before exposure to 10 μM ionomycin for 15 min, and hTOP1 localization was examined by immunofluorescence analysis as described. *MW*, molecular weight; $^{**}p < 0.01$; *ns*, statistically non-significant

the hTOP1^{tr}-containing extract. After ionomycin treatment, the relaxation activity of the si-Vector cell extract was also approximately twofold higher than that of the si-Capn2 #43 cell extract (Fig. 7d). It is generally believed that DNA TOP1 provides the main supercoiling activity in mammalian cells [35]. The enhancement of this relaxation activity of by calpain 2-truncated hTOP1^{tr} is thus likely responsible for the increased relaxation activity of ionomycin-treated cell lysates. Together, these results are consistent with reports showing that the N′-terminal domain of hTOP1 plays a distinct role in its DNA relaxation activity [49, 50]. In addition, our results also suggest the novel regulation of hTOP1 activity by calpain 2.

Calpain 2 protect cells from camptothecin (CPT)-mediated cell killing

TOP1 has also been proven to be an excellent therapeutic target for anticancer therapy [37, 38]. CPT induces cell killing by the formation of a cleavable complex (TOP1 cc),

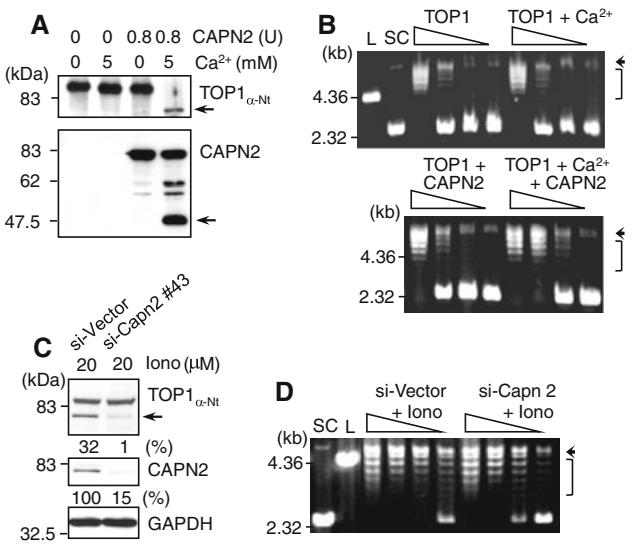

Fig. 7 hTOP1 proteins truncated by calpain 2 exhibit greater relaxation activity than full-length hTOP1. **a** Addition of Ca^{2+} caused proteolysis of both calpain 2 and hTOP1 in vitro. **b** Calpain 2-mediated cleavage enhanced the relaxation activity of hTOP1-containing mixtures. Equal amounts of purified hTOP1 proteins were mixed with Ca^{2+} and/or calpain 2 and the reaction mixtures were incubated for 10 min at room temperature. The relative relaxation activities of reaction mixtures were determined with a twofold serial dilution as described in "Materials and methods". **c**, **d** Ionomycin treatment to calpain 2-proficient cells increased both the proteolysis of hTOP1 and relaxation activity of cellular extracts. HCT116 si-Capn2 #43 and si-Vector cells were treated with 20-μM ionomycin for 15 min, lysed and collected for the immunoblotting analysis (**c**) and relaxation assay (**d**). *Arrows*, truncated hTOP1 or calpain 2 fragments (**a** and **c**); *arrow heads*, nick-from DNA (**b** and **d**); *L*, linearized DNA; *SC*, supercoiled DNA; *Iono*, ionomycin; *Bracket*, DNA topoisomers

Fig. 8 Ca^{2+}-activated calpain 2 cleavage compromised TOP1-mediated cell killing. Cellular exposure to TOP1-targeting camptothecin (CPT, 30 min) resulted in the formation of both the full-length hTOP1 cleavable complex (hTOP1 cc) and truncated hTOP1^{tr}cc in HCT116 cells (**a**). The formation of CPT-induced hTOP1 cc and hTOP1^{tr}cc in the trapping assay is indicated by the disappearance of hTOP1. The levels of full-length (FL) and truncated (Tr) hTOP1 proteins in the ionomycin-treated sample were both taken as 100%. **b** Ionomycin treatment protected cells from the cytotoxic action of CPT. HCT116 cells pre-treated with or without ionomycin (15 min, concentrations as indicated) were co-incubated with CPT (conc. as indicated in figures) for 30 min. The trapping assay and colony formation assay were performed as described in "Materials and methods" to quantify CPT-induced hTOP1 cc formation (**a**) and cell killing ($n = 3$) (**b**). **c**, **d** Calpain 2 is involved in the ionomycin-induced protection from CPT cytotoxicity. HCT116 si-Vector, si-Capn2 #39 or #43 cells were exposed to ionomycin (5 μM) and CPT (5 μM) and cell survival was determined in three independent experiments ($n = 3$). The relative protective effects of ionomycin against CPT-induced cell killing in different cell lines were further quantified using the ratio of survival rates in the presence and absence of ionomycin and represent as "protection folds" in (**d**). **e** The hTOP1 expression level was not affected by the knockdown of calpain 2 in HCT116 cells. **f** CPT induced almost identical formation of hTOP1 cc in HCT116 si-Vector and si-Capn 2 cells. Cells were treated with 5-μM CPT for 30 min and the formation of hTOP1 cc was assayed as described in Fig. 8a ($n = 3$). **g** HT29 cells exhibited the highest basal level of hTOP1 proteolysis among the three colorectal cancer cell lines. **h** Both the Ca^{2+} chelator BAPTA and calpain inhibitor I effectively reduced the endogenous level of hTOP1 proteolysis. HT29 cells incubated with 5-μM ionomycin, 40-μM BAPTA or 5-μM calpain inhibitor I (CAPN Inh I) for 6 h and hTOP1 proteins were assayed as described above. The endogenous level of truncated (Tr) hTOP1 in HT29 cells (*lane* 1) was taken as 100%. Ionomycin treatment induced differential proteolysis of hTOP1 (**i**) and nuclear entry of calpain 2 (**j**) in three different colorectal cell lines. **k** The difference in sensitivity to the CPT-mediated cell killing correlates with a differential hTOP1 proteolysis ability in the three colorectal cancer cell lines. Experiments performed with three colorectal cancer cells, HT29, HCT116, and SW480, were as described above ($n = 3$). *FL*, full-length hTOP1; *Tr*, calpain 2-truncated hTOP1 fragments; $^{**}p < 0.01$; *ns*, statistically non-significant

in which TOP1 is trapped on chromatin and cannot be resolved by SDS-PAGE analysis [37, 38]. As expected, CPT treatment resulted in the disappearance of detectable hTOP1 in the free form (Fig. 8a, compared lane 2–1) since hTOP1 cc is covalently trapped on chromatin DNA. In Fig. 8a, cells were pre-treated with ionomycin (5 μM, 15 min) to generate truncated hTOP1 (hTOP1^{tr}, lane 3). We further showed that CPT treatment induced trapping of hTOP1^{tr}cc (Fig. 8a, compared lane 3 to 4–8) on chromatin DNA in a similar dose-dependent manner. Moreover, we also found that pretreatment with 5-μM ionomycin could protect cells from CPT-mediated cell killing (Fig. 8b). A reduced protective effect of ionomycin on the CPT-induced cell killing was observed in HCT116 si-Capn2 #39 and #43cells (Fig. 8c, d), suggesting the involvement of calpain 2 in this protective effect. Furthermore, calpain 2-deficient HCT116 si-Capn2 #39 and #43 cells were both more sensitive to CPT treatment than HCT116 si-Vector cells

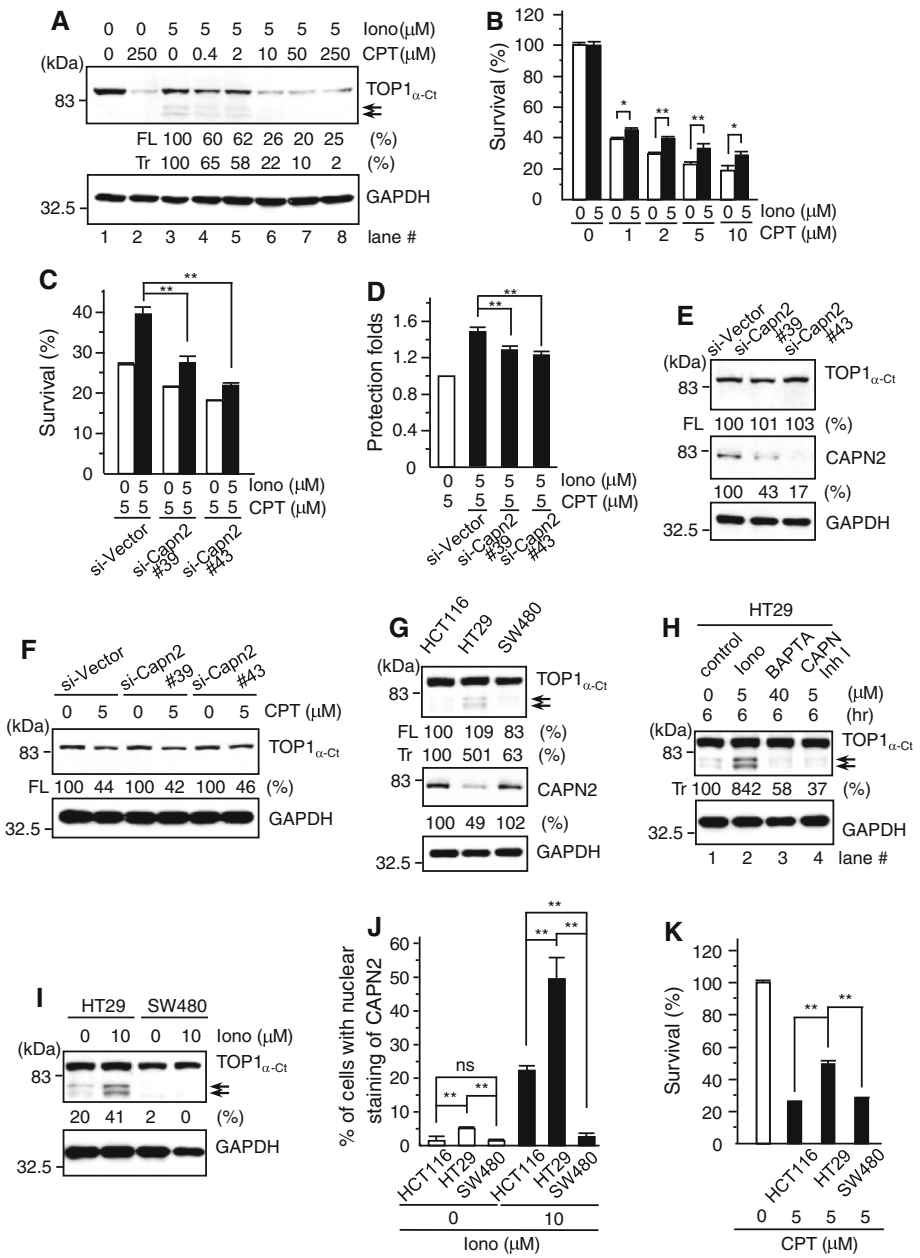

(Fig. 8c). Taken together, our results suggest that calpain 2 might protect cells from CPT-mediated cell killing. This protective effect is not due to change in the expression level of hTOP1 proteins or change in their ability to form hTOP1 cc responding CPT treatment, since hTOP1 levels and CPT-induced hTOP1 cc formation were not altered in HCT116 si-Capn 2 cells (Fig. 8e, f; see quantitative results in Figs. 3h and S2D, $n = 3$).

As stated above, we also found that HT29 cells exhibit an elevated level of endogenous hTOP1 proteolysis (Fig. 1a, b and 8g) suggesting a higher level of calpain 2 activation. Consistent with the notion that calpains and Ca^{2+} are responsible for this higher endogenous level of hTOP1 proteolysis, our results demonstrated that long-term (6-h) treatment with either Ca^{2+} chelator BAPTA or calpain inhibitor I could effectively reduce hTOP1 proteolysis to ~58% (lane 3) and 37% (lane 4) of levels in control cells (lane 1), respectively (Fig. 8h). On the other hand, ionomycin treatment did not induce hTOP1 proteolysis in SW480 cells (Figs. 1a, b; 8i). Thus, the levels of activated endogenous nuclear calpain 2 in the three colorectal cancer cell lines are as follows: HT29 (23.8 ± 4.8%) >> HCT116 (2.3 ± 1.9%) = SW480 (3.0 ± 1.2%; Fig. 1b, $n = 3$). In agreement with this finding, we have also observed that HT29 cells have the highest level of both endogenous basal (5.0 ± 0.4%, $n = 3$) and ionomycin-induced nuclear

immunoreactivity for calpain 2 (49.4. ± 6.3%, $n = 3$) (Figs. 8j and S2E). In agreement with the protective role of calpain 2 in CPT-induced cell killing, we have also found that HT29 cells with the highest endogenous activated calpain 2 are more resistant to CPT-induced cell killing (Fig. 8k). Since the level of hTOP1 is an important sensitivity determinant for CPT, we therefore examined the endogenous levels of hTOP1 in different cell lines and found that HT29 cells contain the highest level of hTOP1 (Fig. S2F, 1.31 ± 0.09-fold, compared to HCT116, $n = 3$, $p < 0.01$). Other cell lines did not exhibit any significant differences in the hTOP1 protein levels compared to HCT116 cells. Next, characteristics of the cleavable complex [37, 38] were examined for those of hTOP1^{tr}cc. First, both hTOP1^{tr}cc and hTOP1 cc on chromatin are released as free hTOP1^{tr} and hTOP1 after a combination of medium reversal and S7 nuclease treatment (Fig. S2G). Together, our results show that hTOP1^{tr}cc is formed upon CPT treatment and exhibits characteristics similar to those of hTOP1 cc.

Discussion

Calpain 1 and calpain 2 are the two calpain proteases that have been extensively studied [11, 13]. Common features are shared by these two proteases include the following: both enzymes require Ca^{2+} for activation (although a great difference in the Ca^{2+} concentration required for activation exists; purified calpain 1 and 2 require concentrations of 3–50 and 400–800 μM of Ca^{2+} for half-maximal activity in vitro), both enzyme exhibit a cytoplasmic localization and both proteases are under inhibitory regulation by calpastatin [22–25]. In addition, common substrates have also been identified via the in vitro cleavage approach [13]. From our in vitro cleavage assay, it is interesting to note that that calpain 2 cleaves hTOP1 more efficiently than calpain 1 with an identical pattern. Experimental results from the cellular fractionation and reconstitution approaches further suggest that this Ca^{2+}-activated hTOP1 proteolysis occurs in the nucleus and that the nuclear membrane limits the access of cytosolic calpains to nuclear hTOP1 proteins. Interestingly, we have found that only calpain 2, but not calpain 1, enters the nucleus upon Ca^{2+} influx. This nucleocytoplasmic shuttling of proteases thus provides a novel regulatory mechanism for the calpain 2-mediated proteolysis of nuclear proteins. In agreement with this notion, nuclear hTOP2β and lamin A/C proteins [51] also cleaved by calpain 2 upon 10 μM ionomycin treatment (data not shown).

How is this calpain 2-mediated proteolysis of hTOP1 regulated? Recent studies suggest that calpain 2 might reside in or translocate into nucleus and then mediate the proteolysis of nuclear proteins [27, 52]. During Ca^{2+}-mediated degeneration of neuron, calpain-mediated changes in the nuclear pore permeability also cause an abnormal nuclear accumulation of large proteins [33]. In our study, we found that both Ca^{2+} and calpastatin regulate the nucleocytoplasmic shuttling of calpain 2 and hTOP1 proteolysis. Calpain catalytic inhibitors only block Ca^{2+}-activated hTOP1 proteolysis but have no effect on the nuclear entry of calpain 2. Therefore, we reason that the ionomycin-induced nuclear entry of calpain 2 is most likely not due to calpain-mediated alterations in nuclear permeability. We have further described a novel regulatory mechanism in which calpastatin regulates calpain 2-mediated proteolysis of nuclear hTOP1, possibly by limiting the nuclear entry of proteases.

Calpains are known to mediate cellular functions through their ability to limitedly cleave substrates involved in different pathways [30, 32, 53]. However, the potential nuclear function(s) of calpains remains largely unknown. Here, we have found that ionomycin treatment, through calpain 2, stimulates proteolysis of hTOP1. In addition, calpain 2 also seems to contribute to the modest protection effect of ionomycin from the CPT-mediated cell killing. It has been reported that the N′-terminal domain plays a direct role in the DNA relaxation and binding ability of hTOP1 [49, 50]. Consistent with this finding, our data show that N′-terminus, calpain 2-truncated hTOP1^{tr} exhibits greater DNA relaxation activity than intact hTOP1, while hTOP1tr still retains the ability forming CPT-DNA-hTOP1^{tr} cleavable complex (hTOP1^{tr}cc). How calpain 2 protects cells from CPT-induced cell killing remains complicated to explain. It is well documented that CPT-sensitivity is determined by several parameters in different cancer cells, and the formation and retention of cleavable complexes on DNA is the key sensitivity/resistance determinant [54, 55]. With regard to the formation and retention of cleavable complexes induced by CPT, our results have revealed that cellular levels of calpain 2 do not affect the levels of hTOP1 proteins. In addition, CPT induced a similar extent of hTOP1^{tr}cc and hTOP1 cc formation (the concentrations trapping 50% of hTOP1 proteins in the form of cleavable complexes are ~3.0 and 3.2 μM for hTOP1 cc and hTOP1^{tr}cc in HCT116 cells, respectively). How calpain 2 proteins affect CPT sensitivity thus remains to be further investigated. In our limited screening using colorectal cancer cell lines, we have found that the basal level of calpain 2-truncated hTOP1^{tr} proteins is higher in HT29 cells and this cellular phenotype also correlates with an elevated level of nuclear calpain 2 staining in HT29 cells. Consistent with the notion that activated calpain 2 protects cells from CPT-mediated cell killing, we have observed that HT29 cells are more resistant to CPT-induced cell killing than two other colorectal cancer cell lines. However, the calpain 2 abundance is decreased in the

HT29 cells. This might be due to the following reasons: reduction in expression at the transcription and/or translation level, increased protein instability and higher activation level of calpain 2. Because HT29 cells also exhibit the highest endogenous cleavage level of hTOP1 by calpain 2 among three cell lines tested, we therefore suggested that the higher activation level of calpain 2 might contribute to the lower calpain 2 abundance in HT29 cells. Since CPT sensitivity is determined by many other parameters in different cancer cell lines and these three colorectal cancer cells are not isogenic, the relative contribution of calpain 2 in CPT sensitivity is therefore experimentally challenging to determine. Nevertheless, it is interesting to note that several recent reports have revealed a potential relationship between elevated calpain activity and poor prognosis in or advanced tumorigenic status of different types of cancer [15–17, 56]. For example, the calpain 2-mediated cleavage of the androgen receptor (AR) has been proposed as a mechanism for androgen independence in prostate cancer [17].

To the best of our knowledge, our study on the calpain 2-mediated hTOP1 proteolysis provides the first demonstration that calpain 2 can effectively cleave nuclear proteins through Ca^{2+}-activated nucleocytoplasmic shuttling of proteases. Notably, the Ca^{2+} concentrations (e.g., 5 mM) that we used in our in vitro study are much higher that the intracellular Ca^{2+} concentrations (nM to μM) and it is thus hard to translate our in vitro findings into in vivo consequences. Nevertheless, considering the potential roles of calpain-mediated cellular destruction in various diseases with elevated intracellular Ca^{2+} levels [2, 3, 7, 9, 57, 58], our discovery may have an important biological and/or clinical implication. It is thus reasonable to speculate that calpain 2-mediated proteolysis of nuclear proteins might also contribute to the pathological progress of diseases found to have altered Ca^{2+} homeostasis. In this regard, the fact that DNA topoisomerases exhibit essential cellular functions supports such a possibility.

Acknowledgments The authors thank Drs. Shu-Chun Teng, Ming-Shyue Lee and Tang-Long Shen (National Taiwan University) for helpful discussions and suggestions. This work has been supported by the Frontier Grant from National Taiwan University as well as by grants from the National Science Council (NSC-96-2320-B-002-081-MY3) and National Health Research Institute (NHRI-EX99-9939NI).

References

1. Bartoli M, Richard I (2005) Calpains in muscle wasting. Int J Biochem Cell Biol 37:2115–2133
2. Tsuji T, Shimohama S, Kimura J, Shimizu K (1998) m-Calpain (calcium-activated neutral proteinase) in Alzheimer's disease brains. Neurosci Lett 248:109–112
3. Vanderklish PW, Bahr BA (2000) The pathogenic activation of calpain: a marker and mediator of cellular toxicity and disease states. Int J Exp Pathol 81:323–339
4. Green KN, LaFerla FM (2008) Linking calcium to Abeta and Alzheimer's disease. Neuron 59:190–194
5. Dargelos E, Brule C, Combaret L, Hadj-Sassi A, Dulong S, Poussard S, Cottin P (2007) Involvement of the calcium-dependent proteolytic system in skeletal muscle aging. Exp Gerontol 42:1088–1098
6. Dargelos E, Poussard S, Brule C, Daury L, Cottin P (2008) Calcium-dependent proteolytic system and muscle dysfunctions: a possible role of calpains in sarcopenia. Biochimie 90:359–368
7. Blomgren K, Zhu C, Wang X, Karlsson JO, Leverin AL, Bahr BA, Mallard C, Hagberg H (2001) Synergistic activation of caspase-3 by m-calpain after neonatal hypoxia-ischemia: a mechanism of "pathological apoptosis"? J Biol Chem 276: 10191–10198
8. Vosler PS, Brennan CS, Chen J (2008) Calpain-mediated signaling mechanisms in neuronal injury and neurodegeneration. Mol Neurobiol 38:78–100
9. Biswas S, Harris F, Dennison S, Singh JP, Phoenix D (2005) Calpains: enzymes of vision? Med Sci Monit 11:RA301–RA310
10. Heidrich FM, Ehrlich BE (2009) Calcium, calpains, and cardiac hypertrophy: a new link. Circ Res 104:e19–e20
11. Croall DE, DeMartino GN (1991) Calcium-activated neutral protease (calpain) system: structure, function, and regulation. Physiol Rev 71:813–847
12. Ono Y, Sorimachi H, Suzuki K (1998) Structure and physiology of calpain, an enigmatic protease. Biochem Biophys Res Commun 245:289–294
13. Goll DE, Thompson VF, Li H, Wei W, Cong J (2003) The calpain system. Physiol Rev 83:731–801
14. Braun C, Engel M, Seifert M, Theisinger B, Seitz G, Zang KD, Welter C (1999) Expression of calpain I messenger RNA in human renal cell carcinoma: correlation with lymph node metastasis and histological type. Int J Cancer 84:6–9
15. Lakshmikuttyamma A, Selvakumar P, Kanthan R, Kanthan SC, Sharma RK (2004) Overexpression of m-calpain in human colorectal adenocarcinomas. Cancer Epidemiol Biomarkers Prev 13:1604–1609
16. Rios-Doria J, Kuefer R, Ethier SP, Day ML (2004) Cleavage of beta-catenin by calpain in prostate and mammary tumor cells. Cancer Res 64:7237–7240
17. Libertini SJ, Tepper CG, Rodriguez V, Asmuth DM, Kung HJ, Mudryj M (2007) Evidence for calpain-mediated androgen receptor cleavage as a mechanism for androgen independence. Cancer Res 67:9001–9005
18. Zatz M, Starling A (2005) Calpains and disease. N Engl J Med 352:2413–2423
19. Cong J, Goll DE, Peterson AM, Kapprell HP (1989) The role of autolysis in activity of the Ca2+ -dependent proteinases (mu-calpain and m-calpain). J Biol Chem 264:10096–10103
20. Kawasaki H, Emori Y, Imajoh-Ohmi S, Minami Y, Suzuki K (1989) Identification and characterization of inhibitory sequences in four repeating domains of the endogenous inhibitor for calcium-dependent protease. J Biochem 106:274–281
21. Maki M, Bagci H, Hamaguchi K, Ueda M, Murachi T, Hatanaka M (1989) Inhibition of calpain by a synthetic oligopeptide corresponding to an exon of the human calpastatin gene. J Biol Chem 264:18866–18869
22. Nishimura T, Goll DE (1991) Binding of calpain fragments to calpastatin. J Biol Chem 266:11842–11850
23. Takano E, Ma H, Yang HQ, Maki M, Hatanaka M (1995) Preference of calcium-dependent interactions between calmodulin-like domains of calpain and calpastatin subdomains. FEBS Lett 362:93–97

24. Hanna RA, Campbell RL, Davies PL (2008) Calcium-bound structure of calpain and its mechanism of inhibition by calpastatin. Nature 456:409–412
25. Moldoveanu T, Gehring K, Green DR (2008) Concerted multipronged attack by calpastatin to occlude the catalytic cleft of heterodimeric calpains. Nature 456:404–408
26. Raynaud F, Carnac G, Marcilhac A, Benyamin Y (2004) m-Calpain implication in cell cycle during muscle precursor cell activation. Exp Cell Res 298:48–57
27. Raynaud F, Marcilhac A, Chebli K, Benyamin Y, Rossel M (2008) Calpain 2 expression pattern and sub-cellular localization during mouse embryogenesis. Int J Dev Biol 52:383–388
28. Tompa P, Buzder-Lantos P, Tantos A, Farkas A, Szilagyi A, Banoczi Z, Hudecz F, Friedrich P (2004) On the sequential determinants of calpain cleavage. J Biol Chem 279:20775–20785
29. Cooray P, Yuan Y, Schoenwaelder SM, Mitchell CA, Salem HH, Jackson SP (1996) Focal adhesion kinase (pp125FAK) cleavage and regulation by calpain. Biochem J 318(Pt 1):41–47
30. Bhatt A, Kaverina I, Otey C, Huttenlocher A (2002) Regulation of focal complex composition and disassembly by the calcium-dependent protease calpain. J Cell Sci 115:3415–3425
31. Carragher NO, Westhoff MA, Fincham VJ, Schaller MD, Frame MC (2003) A novel role for FAK as a protease-targeting adaptor protein: regulation by p42 ERK and Src. Curr Biol 13:1442–1450
32. Franco SJ, Rodgers MA, Perrin BJ, Han J, Bennin DA, Critchley DR, Huttenlocher A (2004) Calpain-mediated proteolysis of talin regulates adhesion dynamics. Nat Cell Biol 6:977–983
33. Bano D, Dinsdale D, Cabrera-Socorro A, Maida S, Lambacher N, McColl B, Ferrando-May E, Hengartner MO, Nicotera P (2010) Alteration of the nuclear pore complex in Ca(2+)-mediated cell death. Cell Death Differ 17:119–133
34. Wang JC (1996) DNA topoisomerases. Annu Rev Biochem 65:635–692
35. Wang JC (2002) Cellular roles of DNA topoisomerases: a molecular perspective. Nat Rev Mol Cell Biol 3:430–440
36. Nitiss JL (2009) DNA topoisomerase II and its growing repertoire of biological functions. Nat Rev Cancer 9:327–337
37. Pommier Y (2009) DNA topoisomerase I inhibitors: chemistry, biology, and interfacial inhibition. Chem Rev 109:2894–2902
38. Li TK, Liu LF (2001) Tumor cell death induced by topoisomerase-targeting drugs. Annu Rev Pharmacol Toxicol 41:53–77
39. Liu LF, Desai SD, Li TK, Mao Y, Sun M, Sim SP (2000) Mechanism of action of camptothecin. Ann N Y Acad Sci 922:1–10
40. Fan JR, Peng AL, Chen HC, Lo SC, Huang TH, Li TK (2008) Cellular processing pathways contribute to the activation of etoposide-induced DNA damage responses. DNA Repair (Amst) 7:452–463
41. Bano D, Young KW, Guerin CJ, Lefeuvre R, Rothwell NJ, Naldini L, Rizzuto R, Carafoli E, Nicotera P (2005) Cleavage of the plasma membrane Na+/Ca2+ exchanger in excitotoxicity. Cell 120:275–285
42. Yang M, Hsu CT, Ting CY, Liu LF, Hwang J (2006) Assembly of a polymeric chain of SUMO1 on human topoisomerase I in vitro. J Biol Chem 281:8264–8274
43. Bharti AK, Olson MO, Kufe DW, Rubin EH (1996) Identification of a nucleolin binding site in human topoisomerase I. J Biol Chem 271:1993–1997
44. Bertipaglia I, Carafoli E (2007) Calpains and human disease. Subcell Biochem 45:29–53
45. Hanna RA, Garcia-Diaz BE, Davies PL (2007) Calpastatin simultaneously binds four calpains with different kinetic constants. FEBS Lett 581:2894–2898
46. Edwards TK, Saleem A, Shaman JA, Dennis T, Gerigk C, Oliveros E, Gartenberg MR, Rubin EH (2000) Role for nucleolin/Nsr1 in the cellular localization of topoisomerase I. J Biol Chem 275:36181–36188
47. Mo YY, Yu Y, Shen Z, Beck WT (2002) Nucleolar delocalization of human topoisomerase I in response to topotecan correlates with sumoylation of the protein. J Biol Chem 277:2958–2964
48. Rallabhandi P, Hashimoto K, Mo YY, Beck WT, Moitra PK, D'Arpa P (2002) Sumoylation of topoisomerase I is involved in its partitioning between nucleoli and nucleoplasm and its clearing from nucleoli in response to camptothecin. J Biol Chem 277:40020–40026
49. Lisby M, Olesen JR, Skouboe C, Krogh BO, Straub T, Boege F, Velmurugan S, Martensen PM, Andersen AH, Jayaram M, Westergaard O, Knudsen BR (2001) Residues within the N-terminal domain of human topoisomerase I play a direct role in relaxation. J Biol Chem 276:20220–20227
50. Palle K, Pattarello L, van der Merwe M, Losasso C, Benedetti P, Bjornsti MA (2008) Disulfide cross-links reveal conserved features of DNA topoisomerase I architecture and a role for the N terminus in clamp closure. J Biol Chem 283:27767–27775
51. Traub P, Scherbarth A, Willingale-Theune J, Paulin-Levasseur M, Shoeman R (1988) Differential sensitivity of vimentin and nuclear lamins from Ehrlich ascites tumor cells toward Ca2+ -activated neutral thiol proteinase. Eur J Cell Biol 46:478–490
52. Tremper-Wells B, Vallano ML (2005) Nuclear calpain regulates Ca2 + -dependent signaling via proteolysis of nuclear Ca2+/calmodulin-dependent protein kinase type IV in cultured neurons. J Biol Chem 280:2165–2175
53. Goni-Oliver P, Lucas JJ, Avila J, Hernandez F (2007) N-terminal cleavage of GSK-3 by calpain: a new form of GSK-3 regulation. J Biol Chem 282:22406–22413
54. Desai SD, Li TK, Rodriguez-Bauman A, Rubin EH, Liu LF (2001) Ubiquitin/26S proteasome-mediated degradation of topoisomerase I as a resistance mechanism to camptothecin in tumor cells. Cancer Res 61:5926–5932
55. Zhang HF, Tomida A, Koshimizu R, Ogiso Y, Lei S, Tsuruo T (2004) Cullin 3 promotes proteasomal degradation of the topoisomerase I-DNA covalent complex. Cancer Res 64:1114–1121
56. Libertini SJ, Robinson BS, Dhillon NK, Glick D, George M, Dandekar S, Gregg JP, Sawai E, Mudryj M (2005) Cyclin E both regulates and is regulated by calpain 2, a protease associated with metastatic breast cancer phenotype. Cancer Res 65:10700–10708
57. Ono Y, Shimada H, Sorimachi H, Richard I, Saido TC, Beckmann JS, Ishiura S, Suzuki K (1998) Functional defects of a muscle-specific calpain, p94, caused by mutations associated with limb-girdle muscular dystrophy type 2A. J Biol Chem 273:17073–17078
58. Samantaray S, Ray SK, Banik NL (2008) Calpain as a potential therapeutic target in Parkinson's disease. CNS Neurol Disord Drug Targets 7:305–312